Current Generation by RF Travelling Field in a Collisional Toroidal Plasma

Masaji FUKUDA

Institute of Plasma Physics, Nagoya University, Nagoya

Abstract

The relation between the current generation by RF travelling field and the accompanied power absorption is studied experimentally in a collisional toroidal plasma. It is confirmed at a low magnetic field that the current is given by the product of the plasma conductivity and an effective electromotive force, which is a new concept introduced on the basis of fluid model; the electromotive force is proportional to the absorbed RF power and inversely proportional to the phase velocity of the travelling field.

§1. Introduction

A direct current generation by RF travelling field was investigated theoretically by several authors[1-6] in connection with the current sustaining of the tokamak plasma. The DC plasma current was already observed to be produced by RF travelling field in a toroidal plasma.[7-12]

Fukuda et al.[13] carried out a series of studies on the current generation in a low toroidal magnetic field and showed the following properties; (1) the current flows in the direction opposite to the RF travelling field, (2) the current depends on the toroidal magnetic field B_t (the current has the maximum at $B_t \sim 100$ G), (3) the dependence on B_t is related to the RF field penetration into the plasma, (4) the current decreases with increasing the filling gas pressure, (5) the electrostatic stray field do not play any essential on the current generation, (6) a reasonable amount of the current is generated by a local excitation even in the case where the line length is shorter than the wavelength.

On the other hand, it was pointed out[5] theoretically that the RF power absorption by electrons is essential for the production of the plasma current by means of RF travelling field. This is because the momentum transfer from the RF field to electrons is accompanied with the RF power absorption. By analyzing the relation between the generated current and the absorbed power in a fluid model, we found that an introduction of a new concept of effective electromotive force is very useful. This concept is related to the power absorption and

the generated current can be interpreted by the effective electromotive force and the plasma conductivity.

In this paper we confirm experimentally this fundamental relation in a collisional plasma at a low magnetic field. In Sec.2 we describe the experimental procedure and in Sec.3 we show experimental results of the current generation. We present in Sec.4 a fluid model for the current generation and introduce a new concept of effective electromotive force. In Sec.5, a comparison between the experiments and the theory is made. It was confirmed experimentally that the electromotive force thus introduced is very useful.

§2. Experimental Procedure

The experiments were performed on a toroidal device of 'Synchromak'. The schematic diagram of the device is shown in Fig.1. The main parameters of the device and experimental conditions are listed in Table (I). Details of the device was described in Ref.(13). An RF travelling field is generated by a transmission line of successive LC circuits which is set up locally on a half of glass discharge tube. The line is terminated by a matching resistor. The phase velocity is 1.9×10^6 m/sec and is equal to the electron thermal velocity of 11 eV. The argon plasma is produced by the RF field itself; argon is used because it is easily ionized.

The generated current is measured by a Rogowskii coil. The loop resistance of the toroidal plasma is measured by applying a weak pulse of induction field, which is generated by a current transformer with iron core (0.02 V.sec); the

loop voltage is 2 ∿ 3 volts. The induction field (a quarter period is 0.5 msec) is applied at 1.5 msec after the RF oscillator is turned on. In Fig.2, we show the time behavior of the toroidal plasma current and loop voltage together with the pulsed perturbation field. We see that the current driven by the travelling field flows stationarily through the duration of RF excitation. The current response to the perturbation field indicates that the toroidal plasma is resistive. The plasma resistance is evaluated from the loop voltage and the induction current with a small correction due to loop inductance of toroidal plasma. We calculate the input power of the perturbation field; that is about 200 W in contrast with the input RF power of several 10 kW. Because of its small power, we do not expect any appreciable modification of the plasma parameters by the application of induction field. In fact, practically no modification was found in the optical observation of the total light from the plasma. It was also observed that the resistance does not change so much during the RF discharge except the initial phase.

The RF power supplied to the line is measured by a directional coupler. The RF power absorbed by the plasma is estimated from the difference between the power supplied to the line and the power dissipated in the dummy resistor. The plasma density is inferred from the fringes of 50 GHz microwave interferometer assuming a uniform density distribution.

3. Experimental Results

3.1. Plasma parameters and RF power absorption.

The electron density of argon plasma is $2 \sim 10 \times 10^{12}$ cm^{-3}. The electron temperature measured by a Langmuir probe is 6 × 13 eV at the center of plasma column. The electron temperature estimated from Spitzer's conductivity[14] is 2 × 4 eV if we assume that the temperature distribution is uniform and the effective charge Z is one (See also Appendix I). In order to exclude this ambiguity of estimation of electron temperature, we calculate the electron collision frequency ν_e more directly from the relation $\nu_e = \eta_p \times (n_e e^2 / m)$ where η_p is the resistivity obtained experimentally from the current response of perturbation field. The collision frequency ν_e ranges $2 \sim 6 \times 10^7$ sec^{-1}, depending on the filling gas pressure. It is comparable with or higher than the wave frequency ($\omega = 1.9 \times 10^7$ rad/sec). The electron-neutral collision frequency ν_{en} is small compared with the wave frequency; $\nu_{en} = 3.3 \times 10^6$ sec^{-1} at $T_e = 10$ eV and $P = 5 \times 10^{-4}$ torr. The ionization frequency ν_{ion} is smaller than the applied RF frequency because the electron temperature is low (Appendix II). Thus the plasma produced by the RF field is in the collisional regime and the main part of ν_e is the electron-ion collisions ν_{ei}.

The RF power absorbed by the plasma is measured by a directional coupler and it is 50 ∿ 80 kW. This power absorption was obtained[13] from the measurement of RF voltages across the condensers of the delay line. Figure 3 shows the distribution of RF voltage for three cases. In the absence of plasma, the voltage distribution along the line was a typical propagating one, though there was a little local

mismatching due to the imperfection of the line arrangement. With plasma, the travelling field was strongly attenuated as passing the line. This attenuation is owing to the power absorption by the plasma. The steady toroidal plasma current is generated by such an RF travelling field as shown in Fig.2.

3.2. Effect of toroidal magnetic field and filling gas pressure.

We measured the generated current I_t, plasma density n_e, plasma resistance R_p and absorbed RF power P_a. In Fig.4, we plot I_t, n_e, R_p and P_a as functions of B_t at a constant filling gas pressure $P = 2.2 \times 10^{-4}$ torr. The generated current I_t has the maximum at about 100 gauss[13] and then the current decreases with increasing B_t monotonically, as shown in Fig.4(a). The plasma density increases with B_t and the plasma resistance decreases with B_t as shown in Fig.4(b) and Fig.4(c), respectively. The absorbed RF power is almost constant against B_t. The joule power dissipated by the DC current is evaluated to be 2.5 kW at I_t = 250 A. Thus we see that it is a small part of the absorbed RF power.

In Fig.5, we plot I_t, n_e, R_p and P_a as functions of the filling gas pressure P at B_t = 130 gauss. The generated current I_t, shown in Fig.5(a), decreases with increasing P. The plasma density increases with P as shown in Fig.5(b). The plasma resistance increases slightly with increasing P as shown in Fig.5(c). The RF power absorbed by the plasma, shown in Fig.5(d), ranges 50 ∿ 80 kW. The dependence on P

was also observed at B_t = 320 gauss and similar dependence of the current and the RF power absorption was obtained.

3.3. Effect of RF power and phase velocity.

We study the effect of RF power by changing the anode voltage E_p of oscillator. In Fig.6, we plot I_t, n_e, R_p and P_a as functions of E_p at B_t = 130 gauss and P = 1.5×10^{-4} torr. The current increases with increasing the absorbed RF power P_a. In this case the increase in plasma density and the decrease in plasma resistance are also seen.

In order to study the effect of phase velocty, three types of the lines having different phase velocities of the travelling field were prepared: $V_p = 1.9 \times 10^6$ m/sec, 1.0×10^6 m/sec and 4.3×10^5 m/sec. The RF frequency is 3.0 MHz for the lines of $V_p = 1.9 \times 10^6$ m/sec, 1.0×10^6 m/sec and 1.5 MHz for $V_p = 4.3 \times 10^5$ m/sec. In Fig.7, the generated current I_t is shown at B_t = 130 gauss and P = 5×10^{-4} torr. The current increases with decreasing V_p.

§4. Force generation and energy absorption.

In this section we study the force generation by RF travelling field and the related power absorption in a collisional plasma ($\omega \lesssim \nu_e$). Here we shall neglect ion motion assuming that ion mass is large enough. In such a plasma, fluid model may be used. The equation of motion for electrons is

$$n_e m \frac{d\mathbb{V}_e}{dt} = - n_e e (\mathbb{E} + \mathbb{V}_e \times \mathbb{B}) - n_e m \nu_e \mathbb{V}_e \quad , \quad (1)$$

where m is the electron mass, V_e is the velocity of the electron fluid, $\hat{\mathbb{E}}$ is the RF electric field and $\mathbb{B}$ is the magnetic field composed of static field B_o and RF field $\hat{\mathbb{B}}$. In the equation ν_e is the collision frequency given by

$$\nu_e = \nu_{ei} + \nu_{en} + \nu_{ion} \quad .$$

The equation of energy for electrons is given by

$$\frac{3}{2} \frac{d(n_e T_e)}{dt} = \langle \mathbb{J} \cdot \mathbb{E} \rangle - \frac{\frac{3}{2} n_e T_e}{\tau_E} \quad , \quad (2)$$

where T_e is the electron temperature, $\mathbb{J}$ is the plasma current density and τ_E is the energy confinement time of the plasma. The time τ_E is governed by the loss mechanism of energy such as diffusion, ionization and radiation. The term $\langle \mathbb{J} \cdot \mathbb{E} \rangle$ means the power absorbed by the plasma.

We consider the electromagnetic field travelling at the phase velocity V_p along the static magnetic field (z-direction). In a steady state we can derive the following force relation using Maxwell's equation,

$$\frac{\langle \mathbb{J} \cdot \mathbb{E} \rangle}{V_p} = n_e m \nu_e V_d \quad ,$$

where V_d is the mean drift velocity of electrons. This relation is also rewritten as

$$\frac{P_a}{J_o} = \eta_p J_{DC} \quad , \quad (3)$$

where $p_a = \langle \mathbb{J} \cdot \mathbb{E} \rangle$ and $J_o = - n_e e V_p$. For energy, we have

$$p_a = \frac{\frac{3}{2} n_e T_e}{\tau_E} \qquad (4)$$

The relation (3) shows that when the power of RF travelling field is absorbed by the plasma, the DC current is generated.

If we integrate eq.(3) along plasma column under the assumption that η_p and J_o are uniform across the plasma column, we have in the right hand side the voltage due to the frictional force for the DC current, or voltage drop in terms of electric circuit. Therefore, we may consider the integral of p_a/J_o to be the effective electromotive force for J_{DC}. Here we may note that with the decrease of collision frequency ν_e, η_p and p_a will tend to zero and then the voltage source representation stated above will become inadequate; in this case the trapped particle model[3] or the current source representation will be suitable. Thus we see that this voltage source representation is applicable for a collision dominant plasma.

In order to understand the mechanism of the current generation due to RF power absorption, we consider a simple model; the RF field is travelling in a cylindrical plasma and the wave frequency ω is lower than ω_{ce}, ω_{pe}, where ω_{ce} is the electron cyclotron frequency and ω_{pe} is the electron plasma frequency. In Fig.8, we illustrate the phase relation among the components of electric field $\tilde{E}$, magnetic field $\tilde{B}$ and plasma current $\tilde{J}$ in a loss free plasma (Appendix III). In this case $\tilde{J}$ and $\tilde{E}$ oscillate out of phase. Thus there is no net absorption of RF power. The force $\tilde{F}_z$ acting

on electrons in the z-direction is given by $\tilde{F}_z = \tilde{\rho}\tilde{E}_z + \tilde{J}_r\tilde{B}_\theta - \tilde{J}_\theta\tilde{B}_r$. For a loss free plasma, the net force is not generated because $\tilde{J}$ and $\tilde{B}$ oscillate out of phase. If the plasma is dissipative, the RF plasma current $\tilde{J}$ oscillates with in phase component relative to RF electric field $\tilde{E}$. The force $\tilde{F}_z$ is distributed in the same direction in every RF magnetic mirror; the force $\tilde{J}_r\tilde{B}_\theta$ and $\tilde{J}_\theta\tilde{B}_r$ are in the same direction. Thus the net force is generated when the RF power of travelling field is absorbed by the plasma.

The RF power absorption may be calculated from eq.(1) or on the basis of dielectric tensor. For $\omega << \omega_{ce}, \omega_{pe}$, we have the following power absorption in the plasma,

$$P_a = \frac{\omega_{pe}^2}{\omega_{ce}^2}\cdot\nu_e\left(\frac{\tilde{E}_r^2 + \tilde{E}_\theta^2}{8\pi}\right) + \frac{\omega_{pe}^2}{\omega^2+\nu_e^2}\cdot\nu_e\,\frac{\tilde{E}_z^2}{8\pi} \qquad (5)$$

From eqs.(3) and (5), the electromotive force is expected to be small in a low collisional plasma ($\nu_e < \omega$) because of small p_a. In this region, however, it will be necessary to consider the collisionless power absorption rather than the collisional damping, and the power absorption given by eq.(5) will be modified[15].

§5. Discussions.

5.1. Force relation

In experiments the RF travelling field produces ionization. The frequency ν_{ion} is, however, low compared with the electron-ion collision frequency ν_{ei}. Thus the ionization does not affect the plasma resistance of eq.(3) so much. In Fig.9,

we replot, from Fig.5, the driving voltage P_a/I_o produced by RF travelling field and the voltage $R_p \times I_t$ due to the frictional force as functions of P at B_t = 130 gauss, where $I_o = J_o S$, S being the cross section area of the plasma column. In Fig.9, P_a/I_o and $R_p \times I_t$ at B_t = 320 gauss is also shown. We see that in both cases the voltages P_a/I_o and $R_p \times I_t$ decrease with increasing P. The voltage P_a/I_o equals to $R_p \times I_t$ within the experimental accuracy. The force relation of eq.(3) is also satisfied for the other phase velocities as shown in Fig.7; the electromotive force increases with decreasing V_p. As for the dependence on P_a, the electromotive force was not observed to increase with P_a though the generated current increased with P_a. This is because the plasma density increases with P_a and the plasma resistance decreases with P_a. Thus we see that the balance is satisfied globally in the ranges of $B_t = 100 \sim 500$ gauss and $\nu_e/\omega = 1 \sim 4$. Therefore the voltage P_a/I_o may be regarded as the effective electromotive force and the current can be estimated from eq.(3).

In the above consideration, we assumed implicitly that the resistivity measured by a pulsed induction field plays the same role for the current driven by the RF travelling field. This assumption may be used in the case where both the current and the conductivity distribution have uniform profiles. Therefore, the experimental results obtained above should be limited in this sense. Estimated correction factor is, however, thought to be smaller than two from the rough observation of current distribution. This smallness of the correction is due to rather uniform temperature profile

which is accompanied with a poor confinement.

5.2. Energy relation.

In this section we consider the power absorption and the energy relation of eq.(4). The RF power absorption by the collisional plasma may be calculated from eq.(5). The RF electric field is estimated using the Maxwell's equation, for the experimental conditions of f = 3 MHz, $n_e \fallingdotseq 5 \times 10^{12}$ cm^{-3}, B_t = 130 gauss, a = 4 cm and $\tilde{B}_z$ = 30 gauss:

$$E_\theta = \frac{\omega \tilde{B}_z}{2} a = 1.0 \text{ KV/m} ,$$

$$E_r = \left(\frac{N^2 - S}{D}\right) E_\theta = 5.0 \text{ KV/m} ,$$

where S and D are components of dielectric tensor used by Stix[15], a is the radius of plasma column and N is the refractive index. If the radial wave number $k_\perp$ is 0.6 cm^{-1} where $k_\perp a = 2.4$ is the solution of $J_o(k_\perp a) = 0$, the electric field $\tilde{E}_r$ is high compared with the field $\tilde{E}_\theta$. The absorbed RF power is calculated to be $\sim$ 50 kW. This RF power agrees fairly with the observed RF power of 50 $\sim$ 80 kW.

In a steady state, the absorbed RF power should balance by the energy losses. We estimate the energy loss due to ionization roughly by using the expression $\nu_{ion} V_i V$, where V_i (= 15.6 eV) is the ionization energy of argon and V is the volume of the plasma. For $\nu_{ion} = 2 \times 10^5$ sec^{-1} and $n_e = 5 \times 10^{12}$ cm^{-3}, the power amounts to 20 kW. As for the energy loss due to diffusion, the power becomes comparable

with the ionization loss. Therefore we see that the input power balances by the energy losses.

We may note that there is the plasma production due to electrostatic stray field $\tilde{E}_z$ underneathe the exciting coil; the field on the surface of the plasma column is strong enough to ionize easily the gas. The plasma thus produced hits the wall and losses the energy. The power dissipated by this mechanism may not produce the effective electromotive force in eq.(3). Experimental results indicate the shielding of this electrostatic field does not cause any significant change in the current generation[13]. Therefore the effect of $\tilde{E}_z$ is not essential in this experiment.

5.3. Wave coupling.

It was observed [13] that the RF field penetrates the plasma as B_t increases. This penetration suggests that the RF travelling field couples with a plasma wave. Using a dielectric tensor of cold, uniform plasma, we obtain the following dispersion relation[15] (whistler mode) for

$$\frac{\omega_{pe}^2}{\omega\,\omega_{ce}} = \frac{c^2}{\omega^2}\, k_{\parallel} \sqrt{k_{\parallel}^2 + k_{\perp}^2} \qquad (6)$$

where $k_\perp$, $k_\parallel$ are the perpendicular and parallel wave number respectively. The equation shows that if $k_\perp$ and $k_\parallel$ are fixed, the plasma density is proportional to the magnetic field B_t. In Fig.10, we show the theoretical dependence of n_e on B_t

together with experimental data of Fig.3(b) (case I) and the data quoted from Fog.2 of Ref.13 (case II). In both cases the plasma density is nearly proportional to B_t. We estimate $k_\perp$ from eq.(6) to be 0.7 $\sim$ 1.5 cm^{-1} for case I and 0.46 cm^{-1} for case II. These values are comparable with the value $k_\perp$= 0.6 cm^{-1} which $k_\perp a$ = 2.4. Therefore we believe that the RF travelling field couples with the proper mode (whistler mode) and then the bell shaped profile of RF field $\tilde{B}_z$ develops.

§5. Conclusion.

We describe a fluid model for the current generation by the RF travelling field and introduce an effective electromotive force p_a/J_o that plays the role of current driving electric field in a collisional plasma. Experiments were carried out in a collisional regime at a low toroidal magnetic field. We measure the generated current, absorbed RF power, plasma density and loop resistance as functions of the toroidal magnetic field, filling gas pressure, supplied RF power and phase velocity. It is observed that the current I_t is produced in such a way that P_a/I_o is equal to $R_p \times I_t$, where R_p is the loop resistance of the toroidal plasma for the joule current and $I_o = -n_e e V_p S$. Since P_a/I_o is the driving voltage and $R_p \times I_t$ is the voltage drop in the model, the experimental results may be summarized on the basis of voltage source model.

Acknoledgements

The author would like to express his sincere thanks to Professor K. Matsuura for his guidance during the course of this work. He is also grateful to Professor Y. Midzuno and Dr. K. Ohkubo for helpful discussions.

Appendix (I) Effect of radial profile of T_e on resistivity.

Here, for simplicity, the radial profile of T_e is assumed to be parabolic ; $T_e = T_{eo} (1 - r^2/a^2)$, where T_{eo} is the electron temperature at the plasma center and a is the radius of the plasma column. The conductivity of the plasma is assumed to be determined only by electron-ion collisions. When the current is driven by the induction electric field, the current is given by

$$I = \int_0^a \sigma E \cdot 2\pi r \, dr = \pi a^2 \sigma_0 E \alpha$$

$$\alpha = \frac{2}{a^2} \int_0^a \left(1 - \frac{r^2}{a^2} \right) r \, dr = \frac{2}{5} \quad ,$$

where α is the correction factor referred to the uniform distribution of T_e. The resistivity is 5/2 times larger than that in the case of uniform profiles. For the loop resistance of 25 mΩ and a = 4 cm, T_{eo} = 7.3 eV (Z = 1) and 10.4 eV (Z = 2). Thus the conductivity temperature T_{eo} is comparable to the temperature measured by the Langmuir probe.

Appendix (II) Estimation of frequency related to ionization.

The frequency related to ionization ν_{ion} is estimated for the plasma in which the electron temperature is lower than the ionization potential. For such a plasma the cross section of ionization may be approximated [16] by

$$\sigma_c = \sigma_{c0} (\varepsilon - \varepsilon_i) \quad ,$$

where ε_i is the ionization energy and ε is the electron energy. This approximation is poor for high energy electrons. However, the effect of these high energy electrons is expected to be small because the number of these electrons is very small. The frequency ν_{ion} is given by

$$\begin{aligned} \nu_{ion} &= n_m \langle \sigma_c v \rangle \\ &= n_m \int_{\varepsilon_i}^{\infty} \sigma_{c0} (\varepsilon - \varepsilon_i) \left(\frac{2\varepsilon}{m_e} \right)^{\frac{1}{2}} \frac{1}{\sqrt{\pi}} \cdot \frac{2\varepsilon^{\frac{1}{2}}}{(T_e)^{\frac{3}{2}}} e^{-\frac{\varepsilon}{T_e}} d\varepsilon \\ &= n_m \sigma_{c0} \langle v_e \rangle (\varepsilon_i + 2T_e) e^{-\frac{\varepsilon_i}{T_e}} \quad , \end{aligned}$$

where n_m is the number of the neutral particl.

For T_e = 10 eV, P = 5×10^{-4} torr, we have $\nu_{ion} = 2 \times 10^5$ sec^{-1}. This frequency is low compared with the wave frequency.

Appendix (III) Phase relation of RF travelling field.

We assume that (1) the RF field is travelling in the z-direction along the static magnetic field, (2) the cylindrical plasma is cold and uniform, (3) ion motion is negligible, (4) the plasma is loss free and (5) $\omega << \omega_{ce}, \omega_{pe}$. In this case the induced electric field $\tilde{D}_r$, $\tilde{D}_\theta$ may be approximated by

$$\tilde{D}_r = - i D \tilde{E}_\theta$$
$$\tilde{D}_\theta = i D \tilde{E}_r$$

where D is the component of the dielectric tensor used by Stix.[15] From Maxwell's equation, we have the following phase relation of RF electric field $\tilde{E}$, RF magnetic field $\tilde{B}$ and RF plasma current $\tilde{J}$ except the coefficients,

$$\tilde{E}_r \propto J_1(k_\perp r) \cos(kz - \omega t)$$
$$\tilde{E}_\theta \propto J_1(k_\perp r) \sin(kz - \omega t)$$
$$\tilde{E}_z \propto J_0(k_\perp r) \sin(kz - \omega t)$$

$$\tilde{B}_r \propto J_1(k_\perp r) \sin(kz - \omega t)$$
$$\tilde{B}_\theta \propto J_1(k_\perp r) \cos(kz - \omega t)$$
$$\tilde{B}_z \propto J_0(k_\perp r) \cos(kz - \omega t)$$

$$\tilde{J}_r \propto J_1(k_\perp r) \sin(kz - \omega t)$$
$$\tilde{J}_\theta \propto J_1(k_\perp r) \cos(kz - \omega t)$$
$$\tilde{J}_z \propto J_0(k_\perp r) \cos(kz - \omega t)$$

where J_m is the Bessel function of the m-th order.

References

1) D.J.H.Wort: Plasma Phys. 13 (1971) 258.

2) R.J.Bickerton: Comments on Mordern Phys. 1 (1972) 95.

3) Y.Midzuno: J. Phys. Soc. Japan 34 (1973) 801.

4) Y.Midzuno: J. Phys. Soc. Japan 38 (1975) 553.

5) R.Klima: Plasma Phys. 15 (1973) 1031.

6) R.Klima and V.L.Sizonenko: Plasma Phys. 15 (1975) 463.

7) P.C.Thonemann, W.T.Cowlig and P.A.Davenprt: Nature 196 (1952) 34.

8) N.A.Borzunov, N.Ya.Kuz'mina. I.Kh.Nevyazhskii, S.M.Osovets, Yu.F.Petrov, B.I.Poyakov, I.A.Popov, K.V.Khodateav and V.P.Shimchuk: Sov. Phys. Doklady 8 (1964) 914.

9) R.A.Demirkhanov, I.Ya.Kadysh, I.S.Fursa and Yu.S. Khadyrev: Sov. Phys.- Tech. Phys. 10 (1965) 174.

10) S.Yoshikawa and H.Yamato: Phys. of Fluids 9 (1966) 1814.

11) K.Hirano, K.Matsuura and A.Mohri: Phys. Letters 36A (1971) 215.

12) S.M.Osovets and I.A.Popov: Fifth European Conf. on Contr. Fusion and Plasma Phys. (Grenoble, France 1972) .

13) M.Fukuda, K.Matsuura, K.Hirano, A.Mohri and M.Fukao: J. Phys. Soc. Japan 41 (1976) 1376.

14) L.Spitzer: Physics of Fully Ionized Gases (Interscience, New York, 1962).

15) T.H.Stix: The Theory of Plasma Waves (McGraw-Hill, New York, 1962).

16) 八田吉典: 気体放電 (近代科学社, 1968).

Figure Captions

Fig. 1. Schematic diagram of Synchromak device

Fig. 2. Time dependence of the generated current I_t and loop voltage U_{cr} together with the pulsed induction field, where B_t = 130 gauss and $P = 4.5 \times 10^{-4}$ torr.

Fig. 3. Distribution of comdenser voltage of the delay line with and without plasma.

Fig. 4. Generated current I_t, plasma density n_e, plasma loop resistance R_p and RF power P_a absorbed by the plasma as functions of the toroidal magnetic field B_t at a constant filling gas pressure $P = 3 \times 10^{-4}$ torr.

Fig. 5. Dependence of I_t, n_e, R_p and P_a on the gas pressure P at B_t = 130 gauss

Fig. 6. Dependence of I_t, n_e, R_p and P_a on the anode voltage E_p of the oscillator at B_t = 130 gauss and $P = 1.5 \times 10^{-4}$torr.

Fig. 7. Dependence of the generated current I_t, voltages P_a/I_o and $R_p \times I_t$ on the phase velocity V_p at B_t = 130 gauss and $P = 6.0 \times 10^{-4}$ torr.

Fig. 8. Phase relations among the components of electric field $\vec{E}$, magnetic field $\vec{B}$ and plasma current $\vec{J}$ in a loss free plasma.

Fig. 9. Voltage $R_p \times I_t$ and driving voltage P_a/I_o produced by the RF travelling field, for parameters of P at B_t = 130 gauss and 320 gauss, where $I_o = J_o S$.

Fig. 10. Comparison between the experimental dependence of n_e on B_t and the dependence predicted from dispersion relation of cold plasma. (●) data of Fig.4(b), (○) data quoted from Fog.2 of Ref.13.

Table (I) Main parameters of the device and experimental conditions.

Discharge tube	
majoy radius	25 cm
minor radius	5 cm
radius of limiter	4 cm
Transmission line	
number of sections	10 ∿ 20
phase velocity	1.9×10^{6} m/sec
capacitance of condensor	1000 pF
Oscillator	
frequency	3.0 MHz
nominal output power	200 kW
pulse width	< 2.5 msec
Iron core	0.02 V.sec
Expermental conditions	
toroidal magnetic field	< 500 G
vertical magnetic field	several gauss
filling gas	argon
filling pressure	$< 3 \times 10^{-3}$ torr

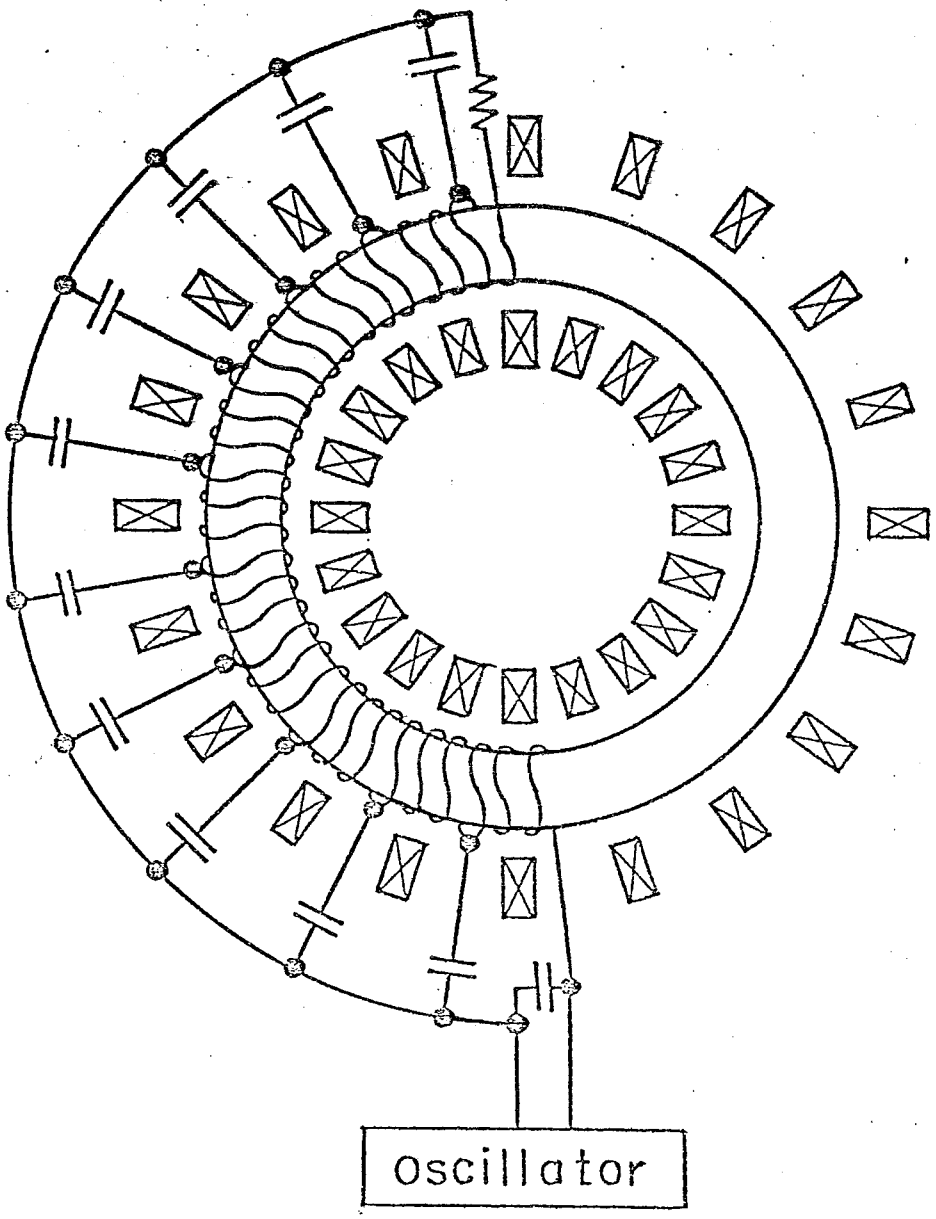

FIG.1.

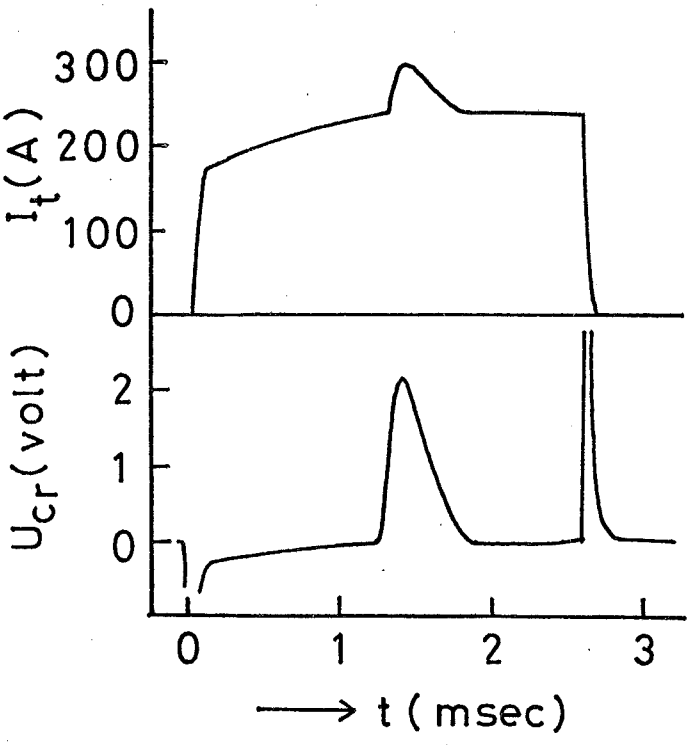

FIG.2.

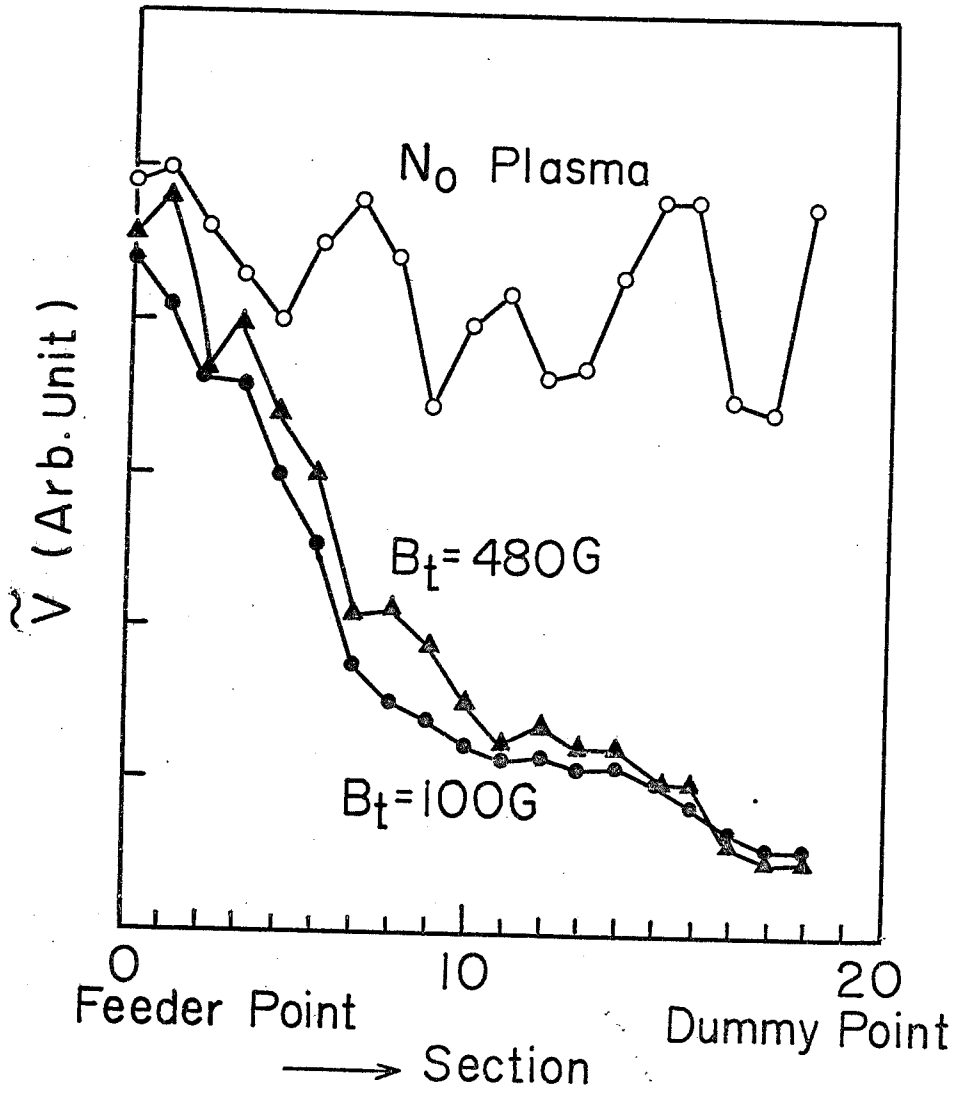
No Plasma
Bt=480G
Bt=100G
Ṽ (Arb. Unit)
0
10
20
Feeder Point
Dummy Point
Section

FIG.3.

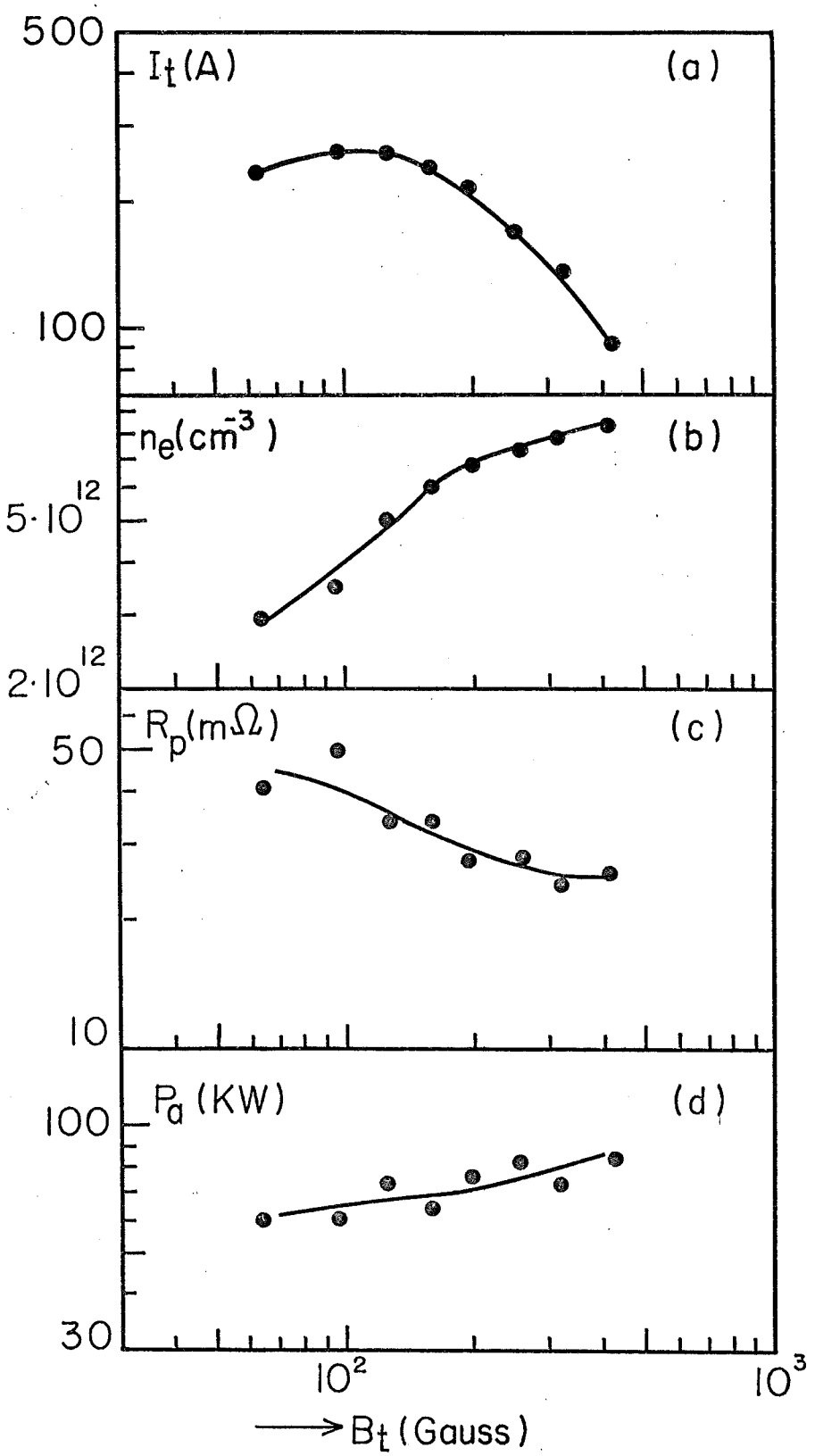
500
I_t(A)
(a)
100
$n_e(cm^{-3})$
(b)
$5\cdot10^{12}$
$2\cdot10^{12}$
$R_p(m\Omega)$
(c)
50
10
P_a (KW)
(d)
100
30
10^2
10^3
B_t (Gauss)

FIG. 4.

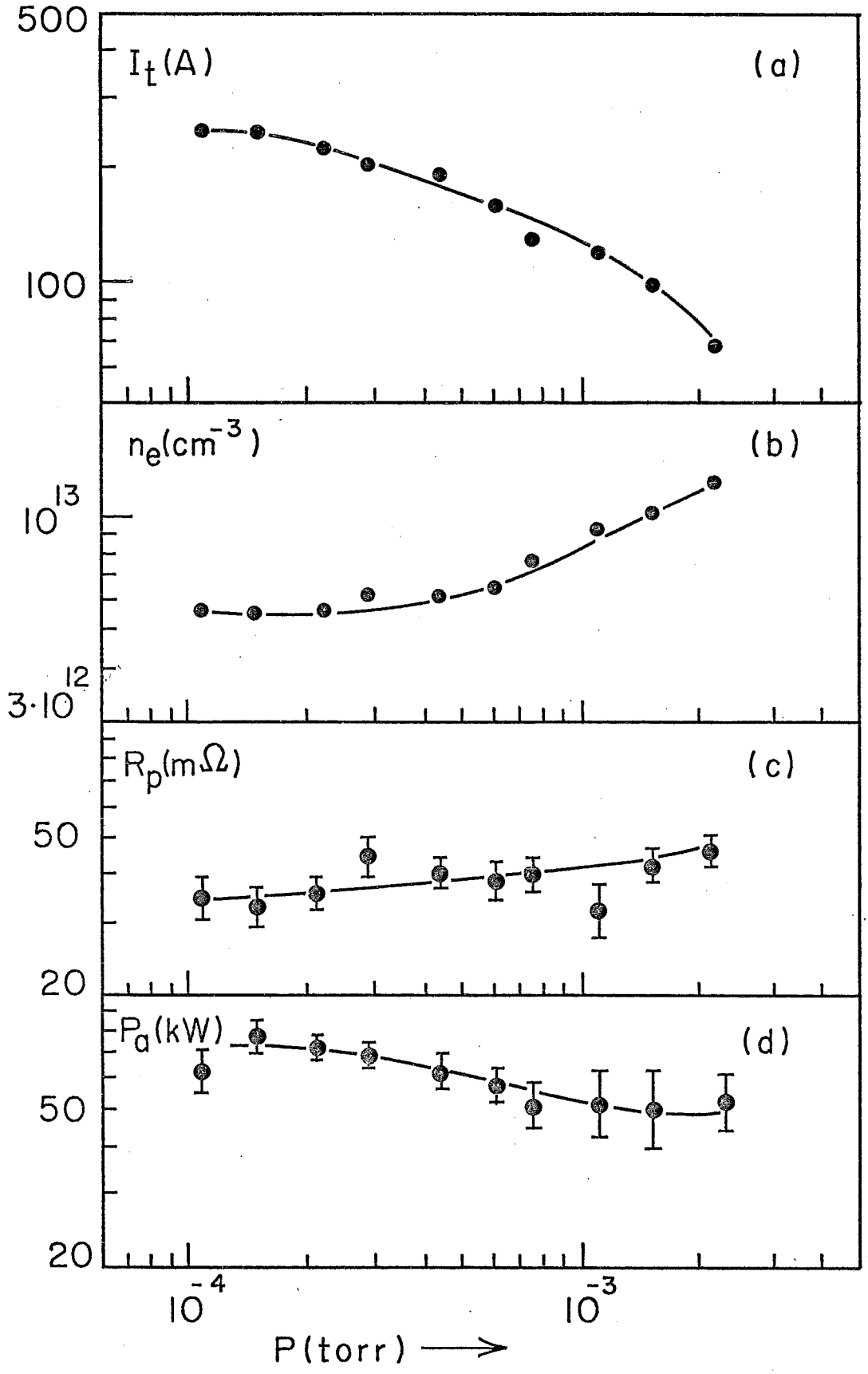
500
I_t(A)
(a)
100
$n_e(cm^{-3})$
(b)
10^{13}
$3\cdot10^{12}$
$R_p(m\Omega)$
(c)
50
20
P_a(kW)
(d)
50
20
10^{-4}
10^{-3}
P(torr) ⟶

FIG.5.

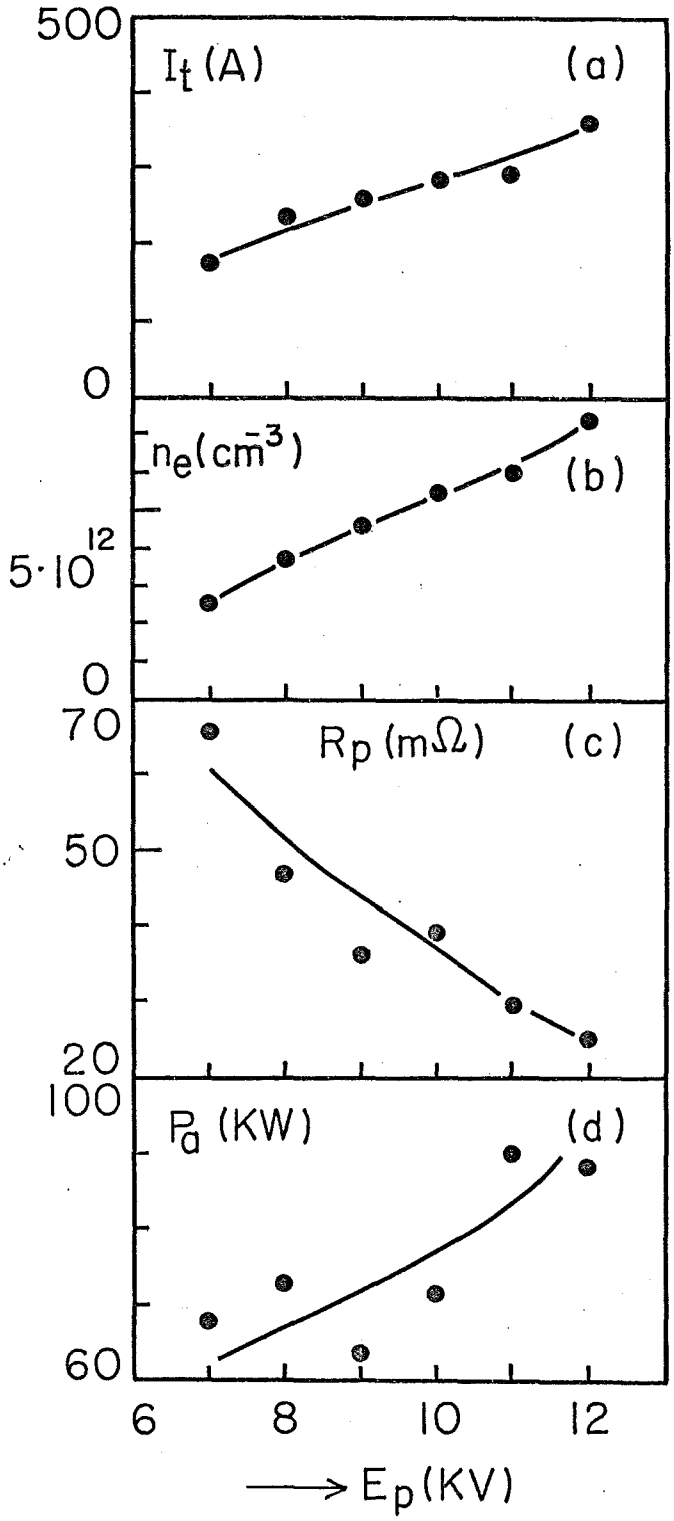
500
I_t (A)
(a)
0
$n_e(cm^{-3})$
(b)
$5 \cdot 10^{12}$
0
70
R_p (mΩ)
(c)
50
20
100
P_a (KW)
(d)
60
6
8
10
12
E_p (KV)

FIG.6.

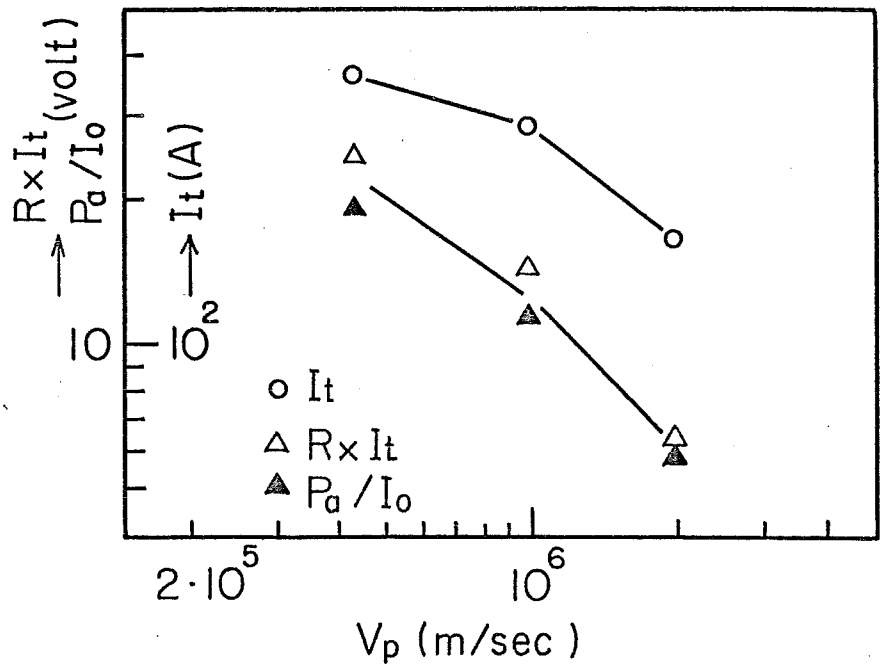

FIG.7.

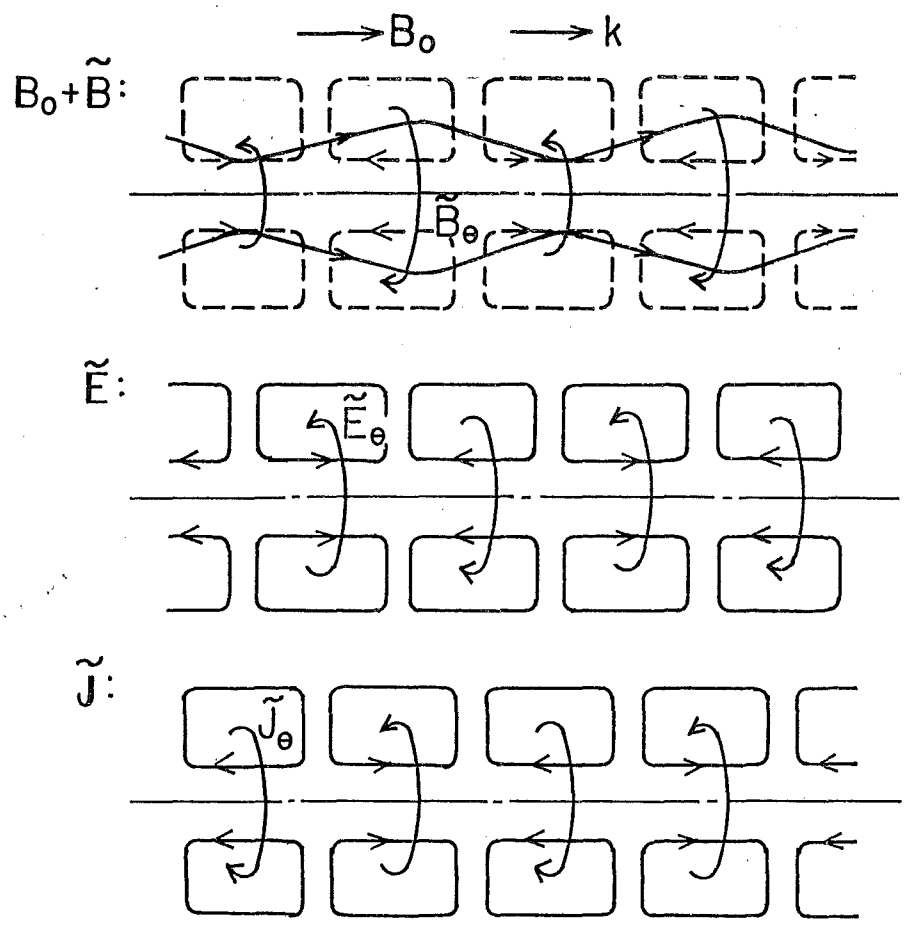
B_0
k
$B_0+\tilde{B}$:
$\tilde{B}_\theta$
$\tilde{E}$:
$\tilde{E}_\theta$
$\tilde{J}$:
$\tilde{J}_\theta$

FIG.8.

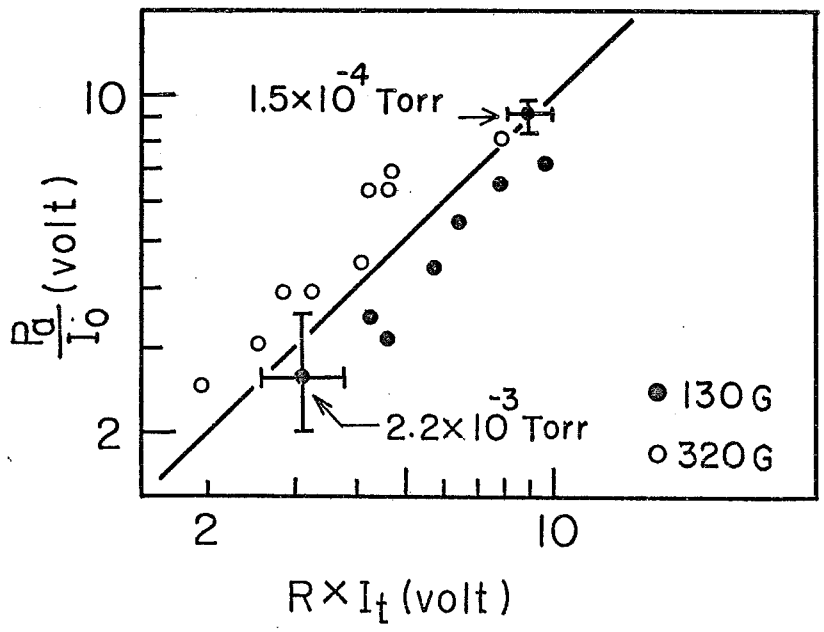

FIG. 9.

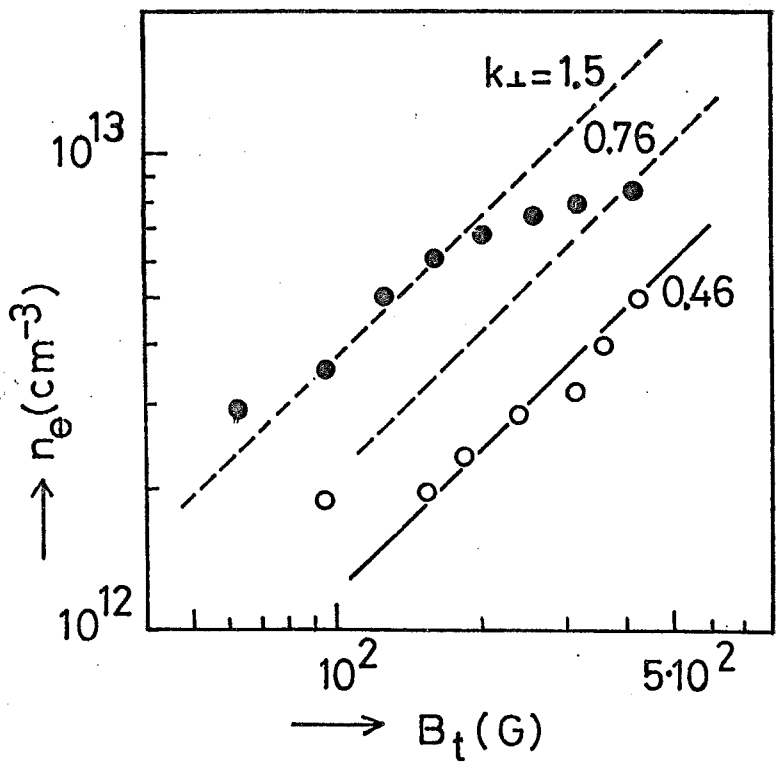
$k_\perp = 1.5$
0.76
0.46
10^{13}
10^{12}
$\longrightarrow n_e(cm^{-3})$
10^2
$5{\cdot}10^2$
$\longrightarrow B_t(G)$

FIG. 10.